Title	Slave mode expansion for obtaining ab initio interatomic potentials
Author(s)	Ai, XY; Chen, Y; Marianetti, CA
Citation	Physical Review B (Condensed Matter and Materials Physics), 2014, v. 90 n. 1, p. 014308
Issued Date	2014
URL	http://hdl.handle.net/10722/214212
Rights	Physical Review B (Condensed Matter and Materials Physics). Copyright © American Physical Society.

Slave mode expansion for obtaining *ab initio* interatomic potentials

Xinyuan Ai (艾馨元)
Department of Physics, Columbia University, New York, New York 10027, USA

Yue Chen (陈粤) and Chris A. Marianetti*
Department of Applied Physics and Applied Mathematics, Columbia University, New York, New York 10027, USA
(Received 8 February 2014; revised manuscript received 11 June 2014; published 31 July 2014)

Here we propose an approach for performing a Taylor series expansion of the first-principles computed energy of a crystal as a function of the nuclear displacements. We enlarge the dimensionality of the existing displacement space and form new variables (i.e., slave modes) which transform like irreducible representations of the point group and satisfy homogeneity of free space. Standard group theoretical techniques can then be applied to deduce the nonzero expansion coefficients *a priori*. At a given order, the translation group can be used to contract the products and eliminate terms which are not linearly independent, resulting in a final set of slave mode products. While the expansion coefficients can be computed in a variety of ways, we demonstrate that finite difference is effective up to fourth order. We demonstrate the power of the method in the strongly anharmonic system PbTe. All anharmonic terms within an octahedron are computed up to fourth order. A proper unitary transformation demonstrates that the vast majority of the anharmonicity can be attributed to just two terms, indicating that a minimal model of phonon interactions is achievable. The ability to straightforwardly generate polynomial potentials will allow precise simulations at length and time scales which were previously unrealizable.

DOI: 10.1103/PhysRevB.90.014308 PACS number(s): 63.20.kg, 71.36.+c, 34.20.Cf

I. INTRODUCTION

While the first-principles computation of the harmonic vibrational properties of crystals with sufficient symmetry is ubiquitous [1–5], the same cannot be said for the anharmonic counterparts. The reasons for this are somewhat indirect. Density functional theory (DFT), within the Born-Oppenheimer approximation [6], can accurately predict the forces and stresses in many classes of materials and therefore could be used to compute both quantum and classical dynamics of the nuclei. However, the scaling of DFT severely restricts the applicability of such a task to very short time scales and small unit cells. Generically, there are a number of different approaches to overcoming this fundamental limitation which exchange accuracy for efficiency, including fully empirical approaches which replace DFT, semiempirical electronic structure approaches [7], and linear scaling DFT [8,9].

One obvious approach which has a long history is to perform a Taylor series expansion of the energy as a function of the nuclear displacements, allowing for extremely high precision up to some order and within some range of neighbors. While such an approach will have obvious limitations (i.e., large deformations, diffusion, etc.), it has a negligible computational cost relative to DFT, allowing length and time scales which could not even be considered within DFT. Furthermore, it has additional appeal in that the expansion coefficients are basic materials properties. Understanding the anharmonic interactions across a broad range of materials will help understand a myriad of materials properties in terms of a low energy model. While the number of anharmonic terms rapidly increases with the order of the expansion, we demonstrate in this work that there is reason to be optimistic that a minimal number of expansion coefficients can capture the bulk of the physics. While the Hubbard and Anderson models have guided us for many years in terms of understanding electronic phenomena in transition-metal oxides and actinide-based materials [10], analogs are clearly needed in the context of the interacting phonon problem.

Some of the early executions of an anharmonic Taylor series expansion based on first-principles calculations were executed by Vanderbilt *et al.* in the context of Si [11] and by Rabe and Vanderbilt *et al.* in the context of ferroelectric materials [12–14]. These approaches were quite successful, correctly capturing the proper ordering of different phases as a function of temperature and even providing quantitatively accurate transition temperatures. In terms of the expansion, a variety of different philosophies were taken in these works. The earliest of these works which focused on Si [11] employed a quartic expansion in terms of bond bending and stretching variables in the spirit of earlier work of Keating [15,16]. Coupling to strain becomes critical in the ferroelectric materials, and an expansion similar to that of Pytte [17] was used by Vanderbilt *et al.* [12] to encode the properties of various perovskites. Subsequent work by Rabe *et al.* [13,14] utilized a novel lattice Wannier function approach [18] to perform an anharmonic expansion (see Ref. [19] for a related approach).

With the continued explosion of computational resources, more recent works have revisited this problem. Esfarjani and Stokes considered the generic Taylor series expansion and all the symmetry constraints that the expansion must satisfy [20]. They then generated a large data set from first-principles calculations and fit the expansion parameters to the data under the symmetry constraints. A number of materials and phenomena have been studied using this approach, including the thermal conductivity in Si [21], half-Heusler compounds [22], and PbTe [23]. Wojdel *et al.* [24] employed a different approach, expanding in displacement differences between pairs of nuclei, similar in spirit to early model calculations [15,16], and they included point symmetry

*chris.marianetti@columbia.edu

by projecting displacement difference polynomials onto the identity representation. Additionally, Wojdel *et al.* explicitly consider strain degrees of freedom and their coupling to local displacements, similar to earlier works in ferroelectric materials.

It is also worth mentioning recent machine learning approaches that have the potential to have significant impact in this space. Behler and Parrinello used a neural network to parametrize the DFT energy [25], and they have achieved impressive results on Na [26,27] and graphite/diamond [28]. These results suggest that appropriate neural networks have the potential to accurately describe structural phase transitions in a broad range of systems, though it is still unclear if they have sufficient resolution to accurately capture phonons and higher derivatives of the energy. Another approach in the context of machine learning is compressive sensing, which has been applied in the context of alloy theory to parametrize cluster expansions [29] and has also shown promise in the context of lattice dynamics.

Despite the great successes of the aforementioned expansions, they have not yet become ubiquitous, perhaps because it is nontrivial to execute the parametrization. Here we introduce an approach which combines many of the advantages of the different methods discussed above. Our approach allows us to circumvent the difficulties of fitting data across multiple orders, builds in all the necessary symmetry from the beginning, is generally applicable, provides a convenient notation to encode our parameters such that others may use them, and in the case of PbTe we show that a physically motivated unitary transformation can reasonably compress hundreds of anharmonic terms into just two.

II. METHOD

A. Background

We will start by considering the total energy of a crystal assuming that the Born-Oppenheimer approximation [6] is valid. The Taylor series expansion of the total energy as a function of the nuclear displacements can be written as follows [20]:

$$V = \sum_{\alpha\beta\mathbf{R}_a\mathbf{R}_b} \Psi^{\alpha\beta}_{\mathbf{R}_a\mathbf{R}_b} u^{(\alpha)}_{\mathbf{R}_a} u^{(\beta)}_{\mathbf{R}_b} + \sum_{\substack{\alpha\beta\gamma \\ \mathbf{R}_a\mathbf{R}_b\mathbf{R}_c}} \Psi^{\alpha\beta\gamma}_{\mathbf{R}_a\mathbf{R}_b\mathbf{R}_c} u^{(\alpha)}_{\mathbf{R}_a} u^{(\beta)}_{\mathbf{R}_b} u^{(\gamma)}_{\mathbf{R}_c} + \sum_{\substack{\alpha\beta\gamma\delta \\ \mathbf{R}_a\mathbf{R}_b\mathbf{R}_c\mathbf{R}_d}} \Psi^{\alpha\beta\gamma\delta}_{\mathbf{R}_a\mathbf{R}_b\mathbf{R}_c\mathbf{R}_d} u^{(\alpha)}_{\mathbf{R}_a} u^{(\beta)}_{\mathbf{R}_b} u^{(\gamma)}_{\mathbf{R}_c} u^{(\delta)}_{\mathbf{R}_d} + \cdots, \quad (1)$$

where Ψ are the direct expansion coefficients; u are the nuclear displacements; $\mathbf{R} = n_1\mathbf{v}_1 + n_2\mathbf{v}_2 + n_3\mathbf{v}_3$ (n_i are integers, $\mathbf{v}_i$ are unit cell vectors); and $\alpha,\beta,\gamma,\delta$ label both the displacement direction (i.e., x,y,z) and the atom within the unit cell. The number of terms dramatically increases as the order increases. Therefore, a condition for this expansion to be useful is locality: The expansion coefficients must decay sufficiently rapidly in some representation for terms beyond quadratic order. This cannot be known *a priori* and only explicit testing could determine the viability of this approach. Symmetry will be crucial both to reduce the number of terms at a given order and to ensure that the expansion is robust for use in simulations. The following symmetries must be satisfied:

(1) The energy must be invariant to all space group operations.

(2) Homogeneity of free space with respect to rigid translation. If the entire crystal is shifted by an arbitrary constant, there cannot be any change in the total energy or its derivatives.

(3) Homogeneity of free space with respect to rigid rotation. If the entire crystal is rotated about some point by an arbitrary amount, there cannot be any change in the total energy or its derivatives.

(4) If the energy function is analytic, the derivatives will be invariant of the order in which they are taken.

These symmetries result in a series of constraints on the expansion coefficients [20]. The central task at hand is to actually compute the derivatives of the energy with respect to the atomic displacements and ensure that they satisfy all of the symmetries.

B. Symmetrized monomial representation

The aforementioned symmetries can be conveniently incorporated via the construction of a monomial representation for each order of the expansion. The strategy will be to build a local space and successively reduce the dimension by incorporating the various symmetries. We begin by simply rewriting the potential in Eq. (1) using a basis of monomials as follows:

$$V = \sum_{\mathbf{R}_a n} \boldsymbol{\Psi}_n \boldsymbol{\xi}^{(n)}_{\mathbf{R}_a} = \sum_{\mathbf{R}_a n} \boldsymbol{\Psi}_n \hat{\boldsymbol{\Gamma}}^{-1}_n \hat{\boldsymbol{\Gamma}}_n \boldsymbol{\xi}^{(n)}_{\mathbf{R}_a}, \quad (2)$$

where n labels the order of the polynomial, $\boldsymbol{\xi}$ is a vector with each entry being a monomial, and $\boldsymbol{\Psi}$ is a vector of the direct expansion coefficients. The dimension of the vector $\boldsymbol{\xi}$ will depend on the range of the interactions Ψ at a given order. If we assume that there is coupling between a set of displacements $\mathcal{S}$ with length $z = |\mathcal{S}|$ at order n, then the dimension of the corresponding monomial representation without symmetry will be given as the k multicombination:

$$\dim(\xi^{(n)}) = \left[\binom{z}{n}\right] = \binom{z+n-1}{n} = \frac{(z+n-1)!}{n!(z-1)!}. \quad (3)$$

The matrix $\hat{\boldsymbol{\Gamma}}_n$ is an invertible linear transformation which can be chosen at each order and will not have an impact on the observables. We can now include the symmetries in the problem, and we begin with the point group symmetry. The only symmetry which we will not consider in this work is homogeneity of free space with respect to rigid rotations, which couples terms between different orders. However, given that we will include point symmetry, we do not believe this will be problematic.

Point symmetry. The monomial representation will in general be reducible, and the standard techniques of group theory [30,31] may be used to decompose the monomial representations into a direct sum of irreducible representations via the proper choice of the matrix $\hat{\boldsymbol{\Gamma}}$. In particular, the point group must be represented by a set of square matrices of dimension $\dim(\xi^{(n)})$, the characters must be constructed for each symmetry class, and the irreducible representations

must be identified and constructed. Given that the potential must be invariant to all point group operations, only representations that transform like the identity representation will yield nonzero expansion coefficients, and these can straightforwardly be found using the projection operator. It should be noted that one could more straightforwardly deduce the number of identity representations by forming a representation of dimension z using the set $\mathcal{S}$ and then use the general formula for the characters of the symmetric product representation [32], though the projection operator will still be used to explicitly construct the terms. Finally, the square matrix $\hat{\mathbf{\Gamma}}$ can be replaced by a rectangular matrix $\hat{\mathbf{\Gamma}}'$ given that representations that are not the identity can be removed, and therefore each row of the rectangular matrix will correspond to a given identity representation of monomials.

$$V = \sum_{\mathbf{R}_a n} \mathbf{\Psi}_n \hat{\mathbf{\Gamma}}'^{-1}_n \hat{\mathbf{\Gamma}}'_n \boldsymbol{\xi}^{(n)}_{\mathbf{R}_a} = \sum_{\mathbf{R}_a n} \mathbf{\Psi}'_n \hat{\mathbf{\Gamma}}'_n \boldsymbol{\xi}^{(n)}_{\mathbf{R}_a}. \tag{4}$$

It is implicit in the above that $\hat{\mathbf{\Gamma}}'^{-1}_n$ is the right inverse of the rectangular matrix $\hat{\mathbf{\Gamma}}'_n$.

Homogeneity of free space. One can remove additional rows of the matrix $\hat{\mathbf{\Gamma}}'_n$ by invoking homogeneity of free space, which dictates that shifting the entire crystal by an arbitrary vector must leave the energy and its derivatives unchanged. In the monomial representation, this condition can be handled in a straightforward fashion. One needs to consider shifting the crystal in the x, y, and z directions by arbitrary constants, in addition to all permutations of combined shifts, which will result in a set of monomial vectors $\{\boldsymbol{\xi}^{(n)}_1, \boldsymbol{\xi}^{(n)}_2, \ldots\}$ which must give zero change in energy. Additionally, the derivatives for each inequivalent atomic displacement in the unit cell can then be considered, and these also must remain invariant with respect to an arbitrary shift. For a given derivative, this must be true independently for contributions from each order. For example, the nth order contribution to the first derivative is given as follows:

$$\frac{\partial V^{(n)}}{\partial u^{(\alpha)}_0} = \mathbf{\Psi}'_n \hat{\mathbf{\Gamma}}'_n \sum_{\mathbf{R}_a} \frac{\partial}{\partial u^{(\alpha)}_0} \boldsymbol{\xi}^{(n)}_{\mathbf{R}_a} = \mathbf{\Psi}'_n \hat{\mathbf{\Gamma}}'_n \boldsymbol{\eta}^{(n,1)}_{\alpha}. \tag{5}$$

The vector $\eta^{(n,1)}$ must then be shifted by arbitrary amounts in the x,y,z directions and all permutations thereof, and it must be required that the change in this component of the derivative is invariant. This procedure is then repeated for all higher order derivatives up to $n-1$. Finally, we will have formed a set of vectors $\mathcal{L}_n = \{\boldsymbol{\xi}^{(n)}_1, \boldsymbol{\xi}^{(n)}_2, \ldots, \boldsymbol{\eta}^{(n,1)}_{\alpha,1}, \boldsymbol{\eta}^{(n,1)}_{\alpha,2}, \ldots\}$. One then proceeds by finding the number of linearly independent vectors in $\mathcal{L}_n$, denoted as $N_{\mathcal{L}_n}$, and then constructing $N_{\mathcal{L}_n}$ vectors from $\mathcal{L}_n$ which span this space. The result will be $N_{\mathcal{L}_n}$ unique constraints due to homogeneity of free space at order n, and this will remove up to $N_{\mathcal{L}_n}$ rows from $\hat{\mathbf{\Gamma}}'_n$, guaranteeing homogeneity of free space. The resulting potential can then be written as follows:

$$V = \sum_{\mathbf{R}_a n} \mathbf{\Psi}''_n \hat{\mathbf{\Gamma}}''_n \boldsymbol{\xi}^{(n)}_{\mathbf{R}_a}. \tag{6}$$

Translation symmetry. While Eq. (6) clearly respects translation symmetry, it is still possible for translational symmetry to eliminate some of the rows in $\hat{\mathbf{\Gamma}}'$ given that the clusters will overlap in general. In order to address this, for a given site $\mathbf{R}_0$ one must sum over all neighboring sites $\mathbf{R}_a$ in Eq. (6) which contain a displacement in $\mathcal{S}_0$, and then determine if all of the identity representations are still linearly independent. Mathematically, we can form the matrix $\hat{\boldsymbol{\mathcal{V}}}_n$ at a given order:

$$\sum_{\mathbf{R}_a} \hat{\mathbf{\Gamma}}''_n \boldsymbol{\xi}^{(n)}_{\mathbf{R}_a}\Big|_{u^{(\alpha)}_{\mathbf{R}_a} \notin \mathcal{S}_0 \to 0} = \hat{\boldsymbol{\mathcal{V}}}_n \boldsymbol{\xi}^{(n)}_0. \tag{7}$$

If the rank of $\hat{\boldsymbol{\mathcal{V}}}_n$ is less than than the number of rows, then there is linear dependence and one or more rows must be combined such that the rank is equivalent to the number of rows. The same row contraction is then performed on $\hat{\mathbf{\Gamma}}''_n$, yielding the final potential:

$$V = \sum_{\mathbf{R}_a n} \mathbf{\Phi}_n \hat{\mathbf{\Gamma}}'''_n \boldsymbol{\xi}^{(n)}_{\mathbf{R}_a}, \tag{8}$$

where we have changed from the symbol $\mathbf{\Psi}_n$ to $\mathbf{\Phi}_n$ in order to emphasize that we have achieved a fully irreducible set of expansion coefficients. It should be noted that $\hat{\mathbf{\Gamma}}'''_n$ is only defined up to an invertible, linear transformation, including rows which could be eliminated by the translation group. Therefore, there is a large degree of freedom in the symmetrization, and we will exploit this in our formulation below.

Illustration of 1D chain. The symmetrized monomial representation outlined above is somewhat abstract and therefore we present a simple example of the monoatomic one-dimensional (1D) chain. The point group is the order two group, which contains only the identity E and the mirror σ [30,31]. The character table for the order two group has two possible irreducible representations: the symmetric and asymmetric irreducible representation denoted as A and B, respectively. We will assume that the range of the coupling is next-nearest neighbor, and therefore the cluster will be composed of the set $\mathcal{S}_0 = \{u_{\bar{1}}, u_0, u_1\}$. Let us consider quadratic order and construct the monomial vector with $[\binom{3}{2}] = 6$ entries:

$$\hat{\boldsymbol{\xi}}^{(2)}_0 = \begin{pmatrix} u^2_{\bar{1}} & u^2_0 & u^2_1 & u_{\bar{1}}u_0 & u_{\bar{1}}u_1 & u_0 u_1 \end{pmatrix}^{\mathsf{T}}. \tag{9}$$

In the absence of symmetry, there would be one independent Ψ parameter for each monomial. Let us now include point symmetry of the cluster $\mathcal{S}$. The standard techniques of group theory can be used to determine that there are four irreducible representations that transform as the identity representation, and the projection operator may be used on seeds composed of individual monomials to construct the following four identity representations:

$$\hat{\mathbf{\Gamma}}'_2 = \begin{pmatrix} 0 & 1 & 0 & 0 & 0 & 0 \\ 1 & 0 & 1 & 0 & 0 & 0 \\ 0 & 0 & 0 & 1 & 0 & 1 \\ 0 & 0 & 0 & 0 & 1 & 0 \end{pmatrix}. \tag{10}$$

We will proceed without normalization as this has no impact on our analysis.

The next step is to enforce homogeneity of free space, and therefore we must construct the vector space $\mathcal{L}$. We will consider both the energy and the force (i.e., only one type of atom and one spatial dimension) under a uniform shift $\delta = 1$,

resulting in two vectors:

$$\mathcal{L} = \begin{Bmatrix} (1 & 1 & 1 & 1 & 1 & 1)^{\mathsf{T}} \\ (2 & 2 & 2 & 2 & 2 & 2)^{\mathsf{T}} \end{Bmatrix}. \tag{11}$$

These two vectors are clearly linearly dependent, indicating that we only have one constraint, and we can proceed with the first vector. There is no unique way to impose the constraint, and we will proceed by eliminating one row via the following transform:

$$\hat{\mathbf{\Gamma}}_2'' = \begin{pmatrix} -\frac{\mathcal{L}\cdot\Gamma_2'^{(2)}}{\mathcal{L}\cdot\Gamma_2'^{(1)}} & 1 & 0 & 0 \\ -\frac{\mathcal{L}\cdot\Gamma_2'^{(3)}}{\mathcal{L}\cdot\Gamma_2'^{(1)}} & 0 & 1 & 0 \\ -\frac{\mathcal{L}\cdot\Gamma_2'^{(4)}}{\mathcal{L}\cdot\Gamma_2'^{(1)}} & 0 & 0 & 1 \end{pmatrix} \cdot \hat{\mathbf{\Gamma}}_2' = \begin{pmatrix} 1 & -2 & 1 & 0 & 0 & 0 \\ 0 & -2 & 0 & 1 & 0 & 1 \\ 0 & -1 & 0 & 0 & 1 & 0 \end{pmatrix},$$

where $\Gamma_2'^{(i)}$ refers to the ith row of $\hat{\mathbf{\Gamma}}_2'$.

The final step is to check and see if the translation group removes any of the rows, and this is done by constructing the matrix $\hat{\mathcal{V}}_2$:

$$\hat{\mathcal{V}}_2 = \begin{pmatrix} 0 & 0 & 0 & 0 & 0 & 0 \\ -2 & -2 & -2 & 2 & 0 & 2 \\ -1 & -1 & -1 & 0 & 1 & 0 \end{pmatrix}. \tag{12}$$

The first row is clearly linearly dependent and therefore the first row of $\hat{\mathbf{\Gamma}}_2''$ may be removed.

The final monomial representation matrix has two rows and can be written as follows:

$$\hat{\mathbf{\Gamma}}_2''' = \begin{pmatrix} 0 & -2 & 0 & 1 & 0 & 1 \\ 0 & -1 & 0 & 0 & 1 & 0 \end{pmatrix}. \tag{13}$$

It should be clear that there is nothing unique about $\hat{\mathbf{\Gamma}}_2'''$, as it can be transformed by any invertible, linear transform without modifying the physics. We will write the final potential at second order as follows:

$$V^{(2)} = \sum_{\mathbf{R}_a} \mathbf{\Phi}_2 \hat{\mathbf{\Gamma}}_2''' \boldsymbol{\xi}^{(2)}_{\mathbf{R}_a}. \tag{14}$$

We have changed from the label $\mathbf{\Psi}$ to $\mathbf{\Phi}$ in order to denote that we are working with the fully irreducible expansion coefficients where all of the symmetry requirements have been built in. The interpretation in this simple case is quite straightforward: Given next-nearest-neighbor coupling at quadratic order, one simply has a nearest-neighbor spring and a next-nearest-neighbor spring. This equivalence can be directly seen by following the same analysis in that scenario.

The preceding outline shows how to build a symmetrized monomial representation, though there is clearly a large degree of flexibility in how to implement this. When moving to more complex scenarios, it would be favorable to have an approach which can more naturally utilize symmetry from the beginning instead of directly working with the monomial representation. In particular, it would be useful to write the monomial representation as a tensor product of symmetric variables which inherently respect the homogeneity of free space. This is exactly what we shall present below, and we shall refer to this as a slave mode expansion. Before giving a formal presentation of the slave mode expansion, it is worth illustrating it in this trivial example. We begin by forming the slave modes, which begins by symmetrizing the cluster variables $\mathcal{S}_0 = \{u_{\bar{1}}, u_0, u_1\}$. One choice of symmetrization is given as follows:

$$\phi_{B^{(1)}} = u_0, \quad \phi_A = u_1 - u_{\bar{1}}, \quad \phi_{B^{(2)}} = u_1 + u_{\bar{1}}. \tag{15}$$

We need to remove the mode which uniformly shifts the cluster, as this would violate homogeneity of free space. In this case, this shift mode corresponds to a linear combination of both B modes, and removing this leaves us with the following two modes:

$$\phi_B = u_1 - 2u_0 + u_{\bar{1}}, \quad \phi_A = u_1 - u_{\bar{1}} \tag{16}$$

These variables already satisfy homogeneity of free space, and they transform like irreducible representations of the point group so it is clear that there are two terms at second order that transform like the identity: ϕ_A^2 and ϕ_B^2. One can construct the matrix $\hat{\mathcal{V}}^{(2)}$ to demonstrate that the translation group does not remove any products, and then one has the irreducible potential:

$$\begin{aligned} V^{(2)} &= \sum_{\mathbf{R}_a} \mathbf{\Phi}_2' \begin{pmatrix} \phi_A^2 \\ \phi_B^2 \end{pmatrix} \\ &= \sum_{\mathbf{R}_a} \mathbf{\Phi}_2' \begin{pmatrix} 1 & 0 & 1 & 0 & -2 & 0 \\ 1 & 4 & 1 & -4 & 2 & -4 \end{pmatrix} \boldsymbol{\xi}^{(2)}_{\mathbf{R}_a} \\ &= \sum_{\mathbf{R}_a} \mathbf{\Phi}_2'' \begin{pmatrix} -\frac{1}{2} & -1 & -\frac{1}{2} & 1 & 0 & 1 \\ -\frac{1}{2} & 0 & -\frac{1}{2} & 0 & 1 & 0 \end{pmatrix} \boldsymbol{\xi}^{(2)}_{\mathbf{R}_a} \\ &= \sum_{\mathbf{R}_a} \mathbf{\Phi}_2 \begin{pmatrix} 0 & -2 & 0 & 1 & 0 & 1 \\ 0 & -1 & 0 & 0 & 1 & 0 \end{pmatrix} \boldsymbol{\xi}^{(2)}_{\mathbf{R}_a}, \end{aligned} \tag{17}$$

where we have expressed the potential in the monomial representation, performed a linear transformation, and then shifted by the first row of $\hat{\mathbf{\Gamma}}_2''$, demonstrating the equivalence to Eq. (14).

C. Slave mode expansion

Building the symmetrized monomial representation would be far more straightforward if the symmetry could be somehow imposed from the beginning. This can be achieved by working with a new set of variables, which can be viewed as enlarging the dimensionality of the system. Instead of using nuclear displacement parameters u, we will introduce so-called *slave modes* ϕ which transform like irreducible representations of the point group and satisfy homogeneity of free space. These slave modes may then be used to expand the potential, and all of the symmetry constraints will be built into the expansion. In terms of the slave modes, the expansion is given as

follows:

$$V = \sum_{\mathbf{R}s}\sum_{\alpha i} \Phi^{s}_{\alpha}\phi^{(i)}_{\alpha\mathbf{R}s}\phi^{(i)}_{\alpha\mathbf{R}s} + \sum_{\mathbf{R}s}\sum_{\substack{\alpha\beta\gamma\\ \zeta,ijk}} \Phi^{s\zeta}_{\alpha\beta\gamma}\Theta^{\zeta,ijk}_{\alpha\beta\gamma}\phi^{(i)}_{\alpha\mathbf{R}s}\phi^{(j)}_{\beta\mathbf{R}s}\phi^{(k)}_{\gamma\mathbf{R}s} + \sum_{\mathbf{R}s}\sum_{\substack{\alpha\beta\gamma\delta\\ \zeta,ijkl}} \Phi^{s\zeta}_{\alpha\beta\gamma\delta}\Theta^{\zeta,ijkl}_{\alpha\beta\gamma\delta}\phi^{(i)}_{\alpha\mathbf{R}s}\phi^{(j)}_{\beta\mathbf{R}s}\phi^{(k)}_{\gamma\mathbf{R}s}\phi^{(l)}_{\delta\mathbf{R}s} + \cdots, \tag{18}$$

where $\alpha,\beta,\gamma,\delta$ label irreducible representations; i,j,k,l label rows of a given irreducible representation; ζ labels a given identity representation within the symmetric product representation; $\mathbf{R}$ is a lattice vector; s labels a cluster associated with a given unit cell; Θ are the Clebsch-Gordan (CG) coefficients; Φ are the irreducible expansion coefficients (as in Sec. II B); and ϕ are the slave modes. It should be noted that cross terms between the clusters with different $\mathbf{R}$ or s are not written as their contribution can be accounted for by simply including larger clusters. The CG coefficients are a group theoretical construct which are independent of any particular application, and these may be straightforwardly computed. However, care must be taken to ensure that a consistent phase convention has been used as there is no unique definition. The slave clusters ϕ are a linear combination of atomic displacements which transform like the irreducible representation of a given point group in the crystal. While we have explicitly written out the quadratic terms using slave modes, we will assume that these will normally be obtained using traditional approaches to compute phonons.

There is a wide degree of flexibility in choosing the slave modes, and the optimum choice may depend on the material and the use of the method. Here we will outline a typical scenario, and specific cases will be dealt with later in the paper.

(1) Determine a cluster of atoms for which the anharmonic terms will be included. This cluster will be associated with a given unit cell (typically primitive), though it could contain atoms which are outside of the unit cell. *At least two atoms must be present in the chosen cluster*. We will refer to this as the slave cluster.

(2) A center of highest symmetry should be identified for the chosen cluster. Each atom in the cluster will have d degrees of freedom, where d is the dimension of space. The displacement vectors should then be projected onto the irreducible representation of the point group.

(3) d linearly independent, symmetrized vectors that correspond to a uniform shift of the cluster need to be eliminated as they would violate homogeneity of free space. The remaining modes are the *slave modes*.

(4) All nontranslation space group operations should be used to determine if translationally inequivalent slave clusters are generated.

(5) The translation group may then be used to generate all translationally equivalent sets.

It may be useful to have multiple types of slave clusters associated with each unit cell, and then the above procedure will be executed for each slave cluster. This will indeed be the case for PbTe.

At this point, we have created a set of variables that respect all of the necessary symmetries, and the tensor product of these variables is a particular realization of the generic monomial representation that was presented in Sec. II B. It should be noted that the slave modes are not simply a change of basis, as they have a higher dimension than degrees of freedom in the crystal. If one wanted to use the slave modes as independent variables, then a constraint would have to be satisfied in order to be sure that the vibrational state is physical. In other words, an arbitrary vector in the space of slave modes will not necessarily have a corresponding vector in the space of displacements. However, this poses no problem in this work as we will always be using the slave modes as dependent variables. One can directly recover Eq. (1) by simply expanding the products of slave modes in Eq. (18).

While it is clear that the slave modes satisfy homogeneity of free space, they also transform like irreducible representations of the point group. This characteristic allows one to trivially determine whether or not a given product of slave modes has a nonzero expansion coefficient. The mathematical question is how many identity representations are contained in the symmetric product of irreducible representations. Fortunately, one can easily construct the characters for the symmetric product representation of a generic representation at a given order. We will denote the direct product using the notation $\otimes$ and the symmetric product as $\odot$ hereafter. In this paper we consider up to fourth order, and the characters for the symmetric product of a given representation are given as follows for second, third, and fourth order [32]:

$$\begin{aligned}
\chi_2(R) &= \tfrac{1}{2}[\chi(R)^2 + \chi(R^2)],\\
\chi_3(R) &= \tfrac{1}{6}[\chi(R)^3 + 3\chi(R^2)\chi(R) + 2\chi(R^3)],\\
\chi_4(R) &= \tfrac{1}{24}[\chi(R)^4 + 8\chi(R)\chi(R^3) + 3\chi(R^2)^2\\
&\quad + 6\chi(R)^2\chi(R^2) + 6\chi(R^4)],
\end{aligned} \tag{19}$$

where R is an element of the group and $\chi(R)$ is the character of R in the given representation. Given that our slave modes already transform like irreducible representations, it is trivial to know *a priori* how many nonzero coefficients a given product will have. If one is dealing with the symmetric product of a single irreducible representation, the general formulas in Eq. (19) can be directly applied. For example, if we are considering the O_h point group and a quartic term $E_g \odot E_g \odot E_g \odot E_g$, the above equation reveals that this yields the direct sum $2E_g \oplus A_{1g}$, and therefore there is only one nonzero expansion coefficient. It is useful to note that one can even more rapidly deduce an upper limit on the number of expansion coefficients by considering the direct product $E_g \otimes E_g \otimes E_g \otimes E_g = 5E_g \oplus 3A_{2g} \oplus 3A_{1g}$, as the symmetric product is a subset of the direct product. In the case of products with multiple types of irreducible representations, or different instances of the same irreducible representation, the symmetric product may be replaced by the direct product. These simple rules are all that is needed. Once the number of nonzero coefficients is determined, the projection operator can be used to construct a corresponding number of linearly independent products of slave modes in that subspace.

D. Slave mode expansion for the 2D square lattice

To illustrate the slave mode expansion we apply it to a two-dimensional (2D) square lattice with one atom per unit cell. We will explore two different choices for slave modes. First, let us consider a slave cluster of two nearest-neighbor atoms (i.e., dimer cluster). In this case, we will choose the center of the cluster as the midpoint of the bond (see Fig. 1, top panel), which will have point group C_{2v} [30]. The representation for the dimer cluster is four dimensional and can be decomposed as $\Gamma = A_1 \oplus A_2 \oplus B_1 \oplus B_2$ (see Fig. 1, top panel). The two normal modes $B_1 \oplus B_2$ correspond to uniform shifts of the cluster, and therefore these modes will be removed, as indicated by the red X, leaving only $A_1 \oplus A_2$. There will be two slave mode products at second order: $\phi^2_{A_1}$ and $\phi^2_{A_2}$. At third order there will be two products: $\phi^3_{A_1}$ and $\phi^2_{A_2}\phi_{A_1}$. At fourth order there will be three products: $\phi^4_{A_1}$, $\phi^4_{A_2}$, and $\phi^2_{A_2}\phi^2_{A_1}$. One can easily proceed to higher orders, but we will remain at quadratic order in the remainder of this example for the sake of simplicity. At this point, one needs to see if any nontranslational symmetry elements will generate a new slave mode cluster which is translationally inequivalent. Clearly, the C_{4v} group at the center of the square will rotate the dimer from a horizontal one to a vertical one. The rotated slave mode products will have identical coefficients. The next step would be to use the translation group to determine if any set of slave mode products is linearly dependent, and this is done by constructing the matrix $\hat{\mathcal{V}}$ as outlined in Sec. II B. In this simple case there is no reduction because dimers only share edges. The conclusion is that there are two coefficients at second order (i.e., Φ_{A_1} and Φ_{A_2}) when considering only nearest-neighbor coupling in the square lattice.

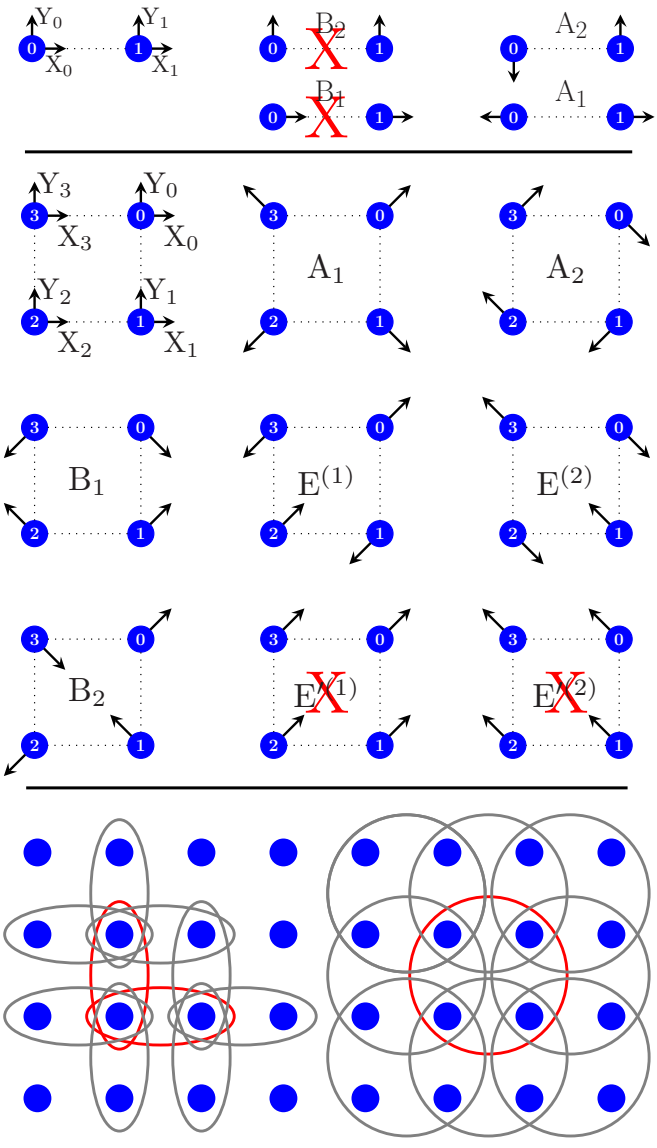

FIG. 1. (Color online) Top panel: Normal modes for the dimer cluster in the square lattice. The red X's designate modes that are removed from the expansion. Middle panel: Normal modes for the square cluster in the square lattice. Bottom panel: A schematic illustrating the summation of overlapping slave modes for the case of the dimer (left) and the square cluster (right). The slave clusters for a central unit cell are illustrated in red while translationally shifted.

The second illustration would be to consider coupling within a square, and this will be carried to second order. In this case the point symmetry group will be C_{4v} [30]. The square cluster representation is eight dimensional and can be decomposed as $\Gamma = A_1 \oplus A_2 \oplus B_1 \oplus B_2 \oplus 2E$ (see Fig. 1, center panel). In this case the E irreducible representation appears twice. One set of the E irreducible representations can be chosen to be shifts of the cluster while the other set will be obtained via orthogonalization. The E representation corresponding to a shift will be removed (as indicated by the red X in Fig. 1), and the slave mode representation will be $A_1 \oplus A_2 \oplus B_1 \oplus B_2 \oplus E$. In this case, there are no nontranslational symmetry elements that will generate translationally inequivalent slave clusters. At second order there will be the following products: $\phi^2_{A_1}, \phi^2_{B_1}, \phi^2_{A_2}, \phi^2_{B_2}, \phi^2_{E^{(1)}} + \phi^2_{E^{(2)}}$. Finally, all slave mode products that overlap a given cluster (see Fig. 1, bottom panel, for an illustration) must be summed over in order to construct $\hat{\mathcal{V}}_2$:

$$\frac{1}{4}\begin{pmatrix} 2 & 2 & -2 & -1 & -1 & 2 & -1 & \cdots \\ 2 & 2 & -2 & -1 & 1 & 2 & -1 & \cdots \\ 2 & -2 & 2 & -1 & 1 & 2 & -1 & \cdots \\ 2 & -2 & 2 & -1 & -1 & 2 & -1 & \cdots \\ 4 & -4 & -4 & 2 & 0 & 4 & 2 & \cdots \end{pmatrix} \begin{pmatrix} x_2^2 \\ x_2x_3 \\ x_2x_1 \\ x_2x_0 \\ x_2y_0 \\ x_3^2 \\ x_3x_1 \\ \vdots \end{pmatrix}. \tag{20}$$

The rank of $\hat{\mathcal{V}}_2$ is 4, and one can show that one of the products $\phi^2_{A_1}, \phi^2_{B_1}, \phi^2_{A_2}, \phi^2_{B_2}$ must be removed. Therefore, there are four expansion coefficients corresponding to the following products: $\phi^2_{A_1}, \phi^2_{B_1}, \phi^2_{B_2}, \phi^2_{E^{(1)}} + \phi^2_{E^{(2)}}$. Typically, one will actually compute the direct expansion coefficients Ψ using DFT, and therefore we will need to relate the slave mode product coefficients Φ to Ψ. At a given order, this can simply be written as a matrix equation, and we illustrate this at second

order for this scenario:

$$\frac{1}{4}\begin{pmatrix} 2 & 2 & 2 & 4 \\ 2 & 2 & -2 & -4 \\ -2 & -2 & 2 & -4 \\ -1 & -1 & -1 & 2 \\ -1 & 1 & -1 & 0 \\ 2 & 2 & 2 & 4 \\ -1 & -1 & -1 & 2 \\ \vdots & \vdots & \vdots & \vdots \end{pmatrix} \begin{pmatrix} \Phi_{A_1} \\ \Phi_{B_1} \\ \Phi_{B_2} \\ \Phi_E \end{pmatrix} = \begin{pmatrix} \Psi_{x_2x_2} \\ \Psi_{x_2x_3} \\ \Psi_{x_2x_1} \\ \Psi_{x_2x_0} \\ \Psi_{x_2y_0} \\ \Psi_{x_3x_3} \\ \Psi_{x_3x_1} \\ \vdots \end{pmatrix}. \quad (21)$$

One needs to compute enough direct expansion coefficients such that the number of linearly independent rows is greater than or equal to the number of columns. If the DFT computations had no imprecisions, one could simply compute as many direct coefficients as slave coefficients, but it is far more robust to create an overdetermined scenario. It is important to note that the above relation is only robust if sufficiently large slave modes are chosen such that they have sufficiently decayed with respect to distance.

III. SLAVE MODE EXPANSION FOR ROCKSALT: PbTe

Here we apply the slave mode expansion to the rocksalt structure of PbTe. We will choose a primitive unit cell having vectors $\mathbf{a_1} = a/2(1,1,0)$, $\mathbf{a_2} = a/2(0,1,1)$, and $\mathbf{a_3} = a/2(1,0,1)$, with a Pb atom at $(0,0,0)$ and a Te atom at $(\frac{1}{2},\frac{1}{2},\frac{1}{2})$ (fractional coordinates; see Fig. 2). The first task is to pick the clusters within which we will retain terms beyond quadratic. There are two natural choices: the Pb-Te dimer and the octahedron (both Pb-centered and Te-centered). We will begin by considering the octahedron as the cluster of choice (see Sec. VI for the dimer), which implies that we will have anharmonic terms within next-nearest neighbor for both Pb and Te. There will be two slave clusters associated with each primitive unit cell, each having O_h point symmetry, and these correspond to atoms connected with bold black lines in Fig. 2. Translationally equivalent clusters can be generated by shifting with the primitive lattice vectors (denoted as green lines in Fig. 2). We now proceed to decompose the displacement vectors into irreducible representations of the O_h point group, and these are shown in Fig. 3 to define the phase conventions which we choose.

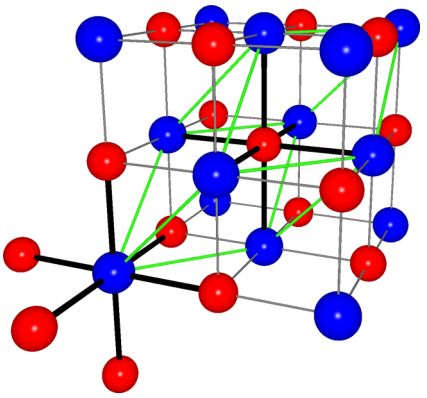

FIG. 2. (Color online) A section of the rocksalt structure. The primitive unit cell is given in green. The two slave clusters associated with the primitive unit cell are denoted by atoms connected with bold lines.

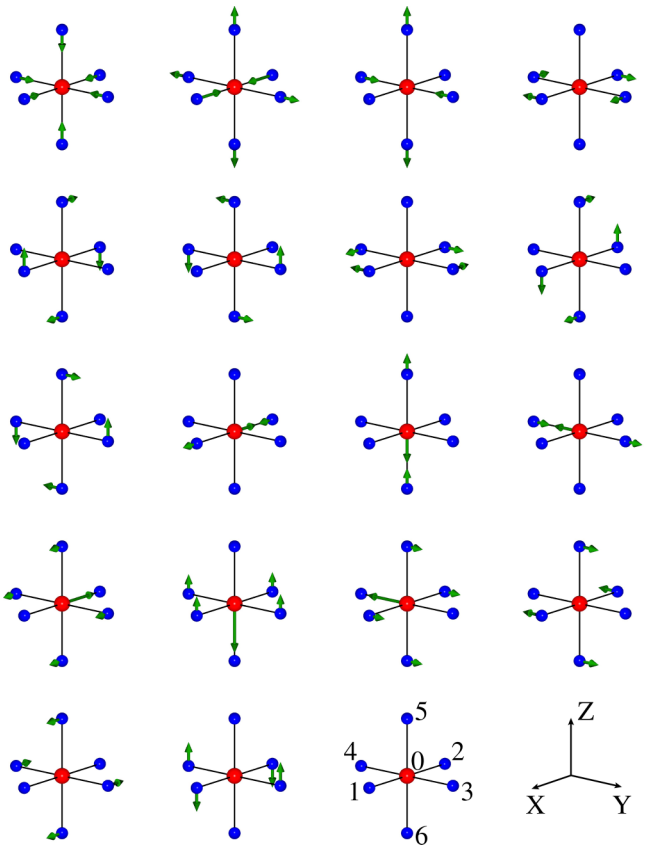

FIG. 3. (Color online) Octahedral modes transforming as the irreducible representations of the point group. The three T_{1u} modes which shift the octahedron have been removed. Reading from left to right and top to bottom, the modes are A_{1g}, E_g, T_{1g}, T_{2g}, $2T_{1u}$, and T_{2u}. Our choice of coordinate system and numbering convention is given in the bottom right. Displacement vectors within a given mode have relative magnitudes of 1, 2, or 4, which can be identified by inspection.

The octahedral slave representation can be decomposed into $\Gamma = A_{1g} \oplus E_g \oplus T_{1g} \oplus T_{2g} \oplus 2T_{1u} \oplus T_{2u}$, where we have removed a T_{1u} manifold which rigidly shifts the octahedron. One can then form the symmetric product representation in a given octahedron, showing that there are 29 nonzero products at third order and 153 nonzero products at fourth order. This will be the case for both Pb- and Te-centered octahedron. Nontranslational symmetry elements will not generate any translationally inequivalent slave clusters. Employing the translation group and constructing the matrices $\hat{\mathcal{V}}_3$ and $\hat{\mathcal{V}}_4$, one can demonstrate that some of the terms are redundant. In particular, two terms will be removed at third order, and four terms will be removed at fourth order. The final result is that there are 56 terms at third order and 302 terms at fourth order, for a total of 358 terms up to fourth order and within next-nearest-neighbor range. The third order products and corresponding coefficients are listed in Table I, while fourth order terms are listed in Table II. It is important

TABLE I. Nonzero third order products and the corresponding expansion coefficients. The second column lists which product vector was used to project the identity and create the Clebsch-Gordan coefficients for each corresponding coefficient Φ. Terms designated N/A were those removed by the translation group.

Product	Phase	Pb-centered Φ	Te-centered Φ
$T_{2g} \otimes 2T_{1u} \otimes T_{2u}$	32, 45	−0.059,−0.048	−0.033,−0.043
$E_g \otimes T_{1g} \otimes T_{1g}$	1	−0.011	0.001
$T_{1g} \otimes T_{1g} \otimes T_{2g}$	16	0.002	−0.002
$A_{1g} \otimes E_g \otimes E_g$	1	0.074	−0.002
$T_{2g} \otimes 2T_{1u} \otimes 2T_{1u}$	38, 59, 84	−0.276,−0.245,−0.524	−0.129,−0.148,−0.284
$T_{1g} \otimes 2T_{1u} \otimes T_{2u}$	45, 54	0.102,−0.084	0.022,−0.025
$A_{1g} \otimes T_{2u} \otimes T_{2u}$	5	−0.01	N/A
$T_{2g} \otimes T_{2g} \otimes T_{2g}$	6	−0.003	0.002
$E_g \otimes 2T_{1u} \otimes T_{2u}$	20, 29	−0.041,0.067	0.008,0.001
$A_{1g} \otimes 2T_{1u} \otimes 2T_{1u}$	4, 15, 22	−1.849,1.288,0.635	−0.282,0.188,0.091
$E_g \otimes T_{2g} \otimes T_{2g}$	14	−0.003	−0.006
$T_{1g} \otimes 2T_{1u} \otimes 2T_{1u}$	6	−0.022	0.006
$E_g \otimes E_g \otimes E_g$	4	−0.035	0.005
$E_g \otimes 2T_{1u} \otimes 2T_{1u}$	4, 22, 51	−2.341,0.941,1.754	0.573,−0.197,−0.449
$T_{2g} \otimes T_{2u} \otimes T_{2u}$	2	0.002	−0.007
$E_g \otimes T_{1g} \otimes T_{2g}$	5	0.018	−0.005
$A_{1g} \otimes T_{2g} \otimes T_{2g}$	9	−0.002	0.006
$A_{1g} \otimes A_{1g} \otimes A_{1g}$	1	0.01	N/A
$A_{1g} \otimes T_{1g} \otimes T_{1g}$	1	−0.011	−0.004
$E_g \otimes T_{2u} \otimes T_{2u}$	10	0.008	0.003

TABLE II. Nonzero fourth order products and the corresponding expansion coefficients. The second column lists which product vector was used to project the identity and create the Clebsch-Gordan coefficients for each corresponding coefficient Φ

Product	Phase	Pb-centered Φ	Te-centered Φ
$E_g \otimes E_g \otimes T_{2g} \otimes T_{2g}$	14, 32	−0.043, −0.034	0.008, 0.01
$T_{2g} \otimes T_{2g} \otimes 2T_{1u} \otimes T_{2u}$	83, 151, 36, 27	0.938, −0.681, 0.031, −0.05	−1.014, 0.742, 0.088, −0.077
$T_{2u} \otimes T_{2u} \otimes T_{2u} \otimes T_{2u}$	1, 5	0.017, 0.003	−0.015, 0.001
$E_g \otimes T_{1g} \otimes T_{1g} \otimes T_{2g}$	35	−0.0	0.003
$T_{1g} \otimes T_{1g} \otimes T_{1g} \otimes T_{2g}$	25	−0.007	−0.001
$A_{1g} \otimes T_{2g} \otimes T_{2g} \otimes T_{2g}$	6	0.001	0.002
$A_{1g} \otimes E_g \otimes T_{1g} \otimes T_{1g}$	14	0.029	−0.01
$T_{1g} \otimes T_{2g} \otimes T_{2g} \otimes T_{2g}$	9	−0.002	0.007
$E_g \otimes E_g \otimes T_{1g} \otimes T_{2g}$	14	−0.121	0.047
$2T_{1u} \otimes 2T_{1u} \otimes 2T_{1u} \otimes 2T_{1u}$	533, 1, 1044 11, 22, 59, 606, 130, 15, 1037, 522	−8.18, 7.405, −3.203, 10.942, 45.45, −10.874, 13.284, −35.053, −2.019, 10.804, −28.53	17.113, 1.528, 7.597, −31.941, −10.505, 30.786, −31.418, 15.514, 7.908, −6.578, N/A
$T_{1g} \otimes T_{1g} \otimes T_{2g} \otimes T_{2g}$	73, 41, 11	0.003, 0.102, −0.005	0.0, −0.102, 0.003
$A_{1g} \otimes A_{1g} \otimes A_{1g} \otimes A_{1g}$	1	0.002	−0.001
$E_g \otimes T_{1g} \otimes T_{2g} \otimes T_{2g}$	47	0.002	0.005
$T_{2g} \otimes T_{2g} \otimes T_{2g} \otimes T_{2g}$	41, 5	0.017, 0.001	−0.017, −0.002
$T_{1g} \otimes T_{1g} \otimes T_{1g} \otimes T_{1g}$	41, 45	0.018, 0.003	−0.014, 0.001
$E_g \otimes T_{1g} \otimes 2T_{1u} \otimes T_{2u}$	54, 108, 1, 8	0.172, −0.297, 0.467, −0.001	−0.11, 0.195, −0.304, −0.006
$E_g \otimes T_{2g} \otimes 2T_{1u} \otimes 2T_{1u}$	89, 16, 146, 102	−1.391, 1.118, −0.416, 0.398	1.716, −0.56, 0.801, −0.685
$2T_{1u} \otimes T_{2u} \otimes T_{2u} \otimes T_{2u}$	18, 83	0.038, 0.054	−0.018, −0.018
$T_{1g} \otimes T_{1g} \otimes 2T_{1u} \otimes 2T_{1u}$	317, 53, 29, 95, 292, 152, 183, 155, 289	2.214, 0.136, 0.021, 0.089, −0.004, 0.833, 0.051, −2.914, −0.013	−1.801, −0.238, −0.05, −0.137, 0.092, −0.584, −0.107, 2.242, −0.046
$A_{1g} \otimes T_{2g} \otimes T_{2u} \otimes T_{2u}$	21	0.007	0.005
$E_g \otimes E_g \otimes E_g \otimes E_g$	4	0.024	−0.01
$E_g \otimes T_{1g} \otimes 2T_{1u} \otimes 2T_{1u}$	16, 192, 111, 167	1.062, 3.955, −2.932, −2.859	−0.674, −2.289, 1.606, 1.627
$A_{1g} \otimes T_{1g} \otimes T_{1g} \otimes T_{2g}$	8	−0.001	0.002
$T_{1g} \otimes T_{1g} \otimes T_{2u} \otimes T_{2u}$	77, 5, 12	0.006, 0.102, −0.005	0.001, −0.098, −0.002
$E_g \otimes T_{2g} \otimes 2T_{1u} \otimes T_{2u}$	17, 99, 71, 21	0.226, 0.207, −0.204, 0.248	−0.069, 0.098, 0.198, −0.363

TABLE II. (*Continued*.)

Product	Phase	Pb-centered Φ	Te-centered Φ
$E_g \otimes E_g \otimes T_{1g} \otimes T_{1g}$	9, 28	0.071, −0.106	−0.026, 0.039
$A_{1g} \otimes T_{1g} \otimes 2T_{1u} \otimes T_{2u}$	10, 40	−0.263, −0.359	0.071, 0.118
$A_{1g} \otimes T_{2g} \otimes 2T_{1u} \otimes 2T_{1u}$	102, 38, 41	−0.905, 0.882, −1.902	0.675, −0.724, 1.459
$T_{1g} \otimes T_{1g} \otimes 2T_{1u} \otimes T_{2u}$	83, 39, 107, 74	0.986, −0.009, 0.025, −0.718	−0.918, 0.02, −0.027, 0.662
$E_g \otimes T_{2g} \otimes T_{2u} \otimes T_{2u}$	29	−0.003	0.002
$2T_{1u} \otimes 2T_{1u} \otimes 2T_{1u} \otimes T_{2u}$	30, 540, 280, 306, 142, 7	2.355, −1.842, −0.811, 4.857, −3.446, −1.88	−8.661, 4.674, 3.853, −10.649, 6.226, 4.979
$A_{1g} \otimes A_{1g} \otimes 2T_{1u} \otimes 2T_{1u}$	8, 11, 29	0.598, −0.725, 0.145	0.078, −0.158, 0.096
$A_{1g} \otimes E_g \otimes E_g \otimes E_g$	1	0.03	0.0
$A_{1g} \otimes E_g \otimes T_{2u} \otimes T_{2u}$	5	0.028	−0.005
$A_{1g} \otimes E_g \otimes T_{1g} \otimes T_{2g}$	10	0.17	−0.06
$A_{1g} \otimes E_g \otimes 2T_{1u} \otimes 2T_{1u}$	29, 54, 51	−2.974, −3.915, 2.377	0.315, 0.165, 0.021
$A_{1g} \otimes A_{1g} \otimes T_{1g} \otimes T_{1g}$	5	−0.018	0.001
$A_{1g} \otimes T_{1g} \otimes 2T_{1u} \otimes 2T_{1u}$	89	0.831	−0.347
$E_g \otimes E_g \otimes 2T_{1u} \otimes 2T_{1u}$	130, 47, 72, 11, 15 116	−0.093, −2.737, −0.91, −0.678, −0.85, 1.64	0.255, 0.112, −0.052, −0.397, 0.175, N/A
$A_{1g} \otimes A_{1g} \otimes T_{2g} \otimes T_{2g}$	1	−0.013	N/A
$A_{1g} \otimes T_{2g} \otimes 2T_{1u} \otimes T_{2u}$	10, 23	−0.146, −0.237	0.108, 0.16
$E_g \otimes E_g \otimes T_{2u} \otimes T_{2u}$	18, 36	0.043, −0.037	−0.009, 0.007
$A_{1g} \otimes E_g \otimes 2T_{1u} \otimes T_{2u}$	34, 20	0.754, −0.283	−0.344, 0.133
$T_{1g} \otimes T_{2g} \otimes 2T_{1u} \otimes T_{2u}$	83, 74, 22, 143, 155, 72, 79, 113	1.913, −1.372, −0.02, 0.04, −0.07, −0.004, −0.056, −0.026	−2.0, 1.461, −0.015, −0.052, 0.039, −0.027, 0.029, 0.038
$E_g \otimes T_{1g} \otimes T_{2u} \otimes T_{2u}$	2	−0.001	−0.001
$T_{2g} \otimes T_{2g} \otimes T_{2u} \otimes T_{2u}$	24, 77, 41	−0.001, 0.003, 0.098	−0.007, −0.002, −0.105
$2T_{1u} \otimes 2T_{1u} \otimes T_{2u} \otimes T_{2u}$	198, 99, 28, 264, 135, 72, 87, 20, 261	−0.194, −3.438, 0.63, 0.415, −0.47, 1.251, 0.813, 0.409, 2.36	0.326, 3.335, −0.834, 0.041, 0.531, −1.225, 0.133, 0.09, −2.28
$T_{2g} \otimes T_{2g} \otimes 2T_{1u} \otimes 2T_{1u}$	306, 196, 1, 317, 66, 8, 310, 162, 45	−2.88, −0.216, 0.857, 2.154, −0.093, −0.048, −0.015, 0.067, −0.118	2.73, −0.047, −0.8, −2.083, −0.056, −0.106, 2.73, −0.047, −0.8, −2.083, −0.125, 0.226, N/A
$T_{1g} \otimes T_{2g} \otimes 2T_{1u} \otimes 2T_{1u}$	15, 95, 120, 221, 18, 324, 117	3.295, −0.036, −0.071,−0.081, −7.9, −5.024, 0.104	−3.6, −0.228, −0.166, −0.148, 8.646, 5.441, 0.098
$A_{1g} \otimes A_{1g} \otimes T_{2u} \otimes T_{2u}$	1	−0.014	−0.0
$A_{1g} \otimes E_g \otimes T_{2g} \otimes T_{2g}$	9	0.018	−0.013
$T_{1g} \otimes T_{2g} \otimes T_{2u} \otimes T_{2u}$	60, 73	0.002, −0.202	−0.005, 0.205
$A_{1g} \otimes A_{1g} \otimes E_g \otimes E_g$	4	0.027	0.003
$E_g \otimes E_g \otimes 2T_{1u} \otimes T_{2u}$	6, 29	−0.288, −0.326	−0.008, 0.021

to note the phase convention we chose in constructing the Clebsch-Gordan coefficients. The vectors in each product subspace are labeled from $1 \cdots N$ when taking the following ordering:

$$|1,0,0,0,0,\cdots\rangle, |0,1,0,0,0,\cdots\rangle, \cdots \tag{22}$$

where each of the above vectors is a direct product of the given vectors of the respective irreducible representations listed in the table. The corresponding identity representation is obtained by taking the product vector with the designated phase number in the second column and projecting onto the identity representation.

IV. COMPUTING EXPANSION COEFFICIENTS FOR PbTe

Having determined the slave mode expansion up to fourth order and within next-nearest neighbor, the slave mode coefficients must be computed. In general, there are many approaches to execute this task. First, as described above, we will assume that the harmonic terms have been computed using traditional approaches for computing phonons from first principles, such as density functional perturbation theory [1] or finite displacement supercell approaches [2,3]. Therefore, we are only concerned with computing the third and fourth order terms. An obvious approach would be to construct a large data set of distorted structures in the anharmonic regime and compute the corresponding energies using DFT. This data set may then be used to fit the slave mode expansion coefficients using standard procedures. The drawback of such an approach is that one is always faced with the problems of overfitting or including data which is beyond fourth order. While there are standard statistical methods to address such problems, we believe other approaches are likely more straightforward. Another approach would be to compute individual expansion coefficients for a given monomial [i.e., Eq. (1)], analogous to what is done for the harmonic case in phonons. One could either use the $2N + 1$ theorem from density functional perturbation theory [33–35], or a supercell approach using

finite displacements could be used. We will opt for the latter in this work.

The computed direct expansion terms are only of limited use given that small errors within the numerical implementation of DFT will prevent the computed direct terms from satisfying all the necessary symmetries. However, there is a linear relation between the slave mode coefficients and the direct expansion coefficients [see Eq. (21) for an example]. Therefore, one simply needs to compute enough direct coefficients such that the slave mode coefficients are uniquely defined. In the case of PbTe, we will need to compute at least 56 monomial coefficients at third order and 302 at fourth order. In practice, it is desirable to compute more than the minimum number to minimize the effects of error within the DFT finite difference calculations.

These linear relations will properly average out noise from the direct coefficients and enforce all symmetry relations. What should be apparent is that these relations assume a truncation in the range of the slave modes. This is clearly an approximation which relies on a sufficient degree of locality in order to be accurate, and we will show that our truncation of an octahedron for PbTe is reasonable. The other major potential source of error is the convergence of the direct finite difference terms which will be dealt with below. While it would be desirable to directly compute the slave mode coefficients, this is not straightforward as the slave modes are not orthogonal.

A. DFT runs and finite difference

As outlined above, the direct expansion coefficient will be computed with finite difference. Given that the forces are known from the Hellman-Feynman theorem [36], the first derivatives will all be known for a given DFT computation. Using a central finite difference, a derivative containing up to four variables can generically be written:

$$\begin{aligned}
&\frac{\partial^n E}{\partial q_\alpha^h \partial q_\beta^i \partial q_\gamma^j \partial q_\delta^k} \\
&= \frac{\partial^{n-1} F_\alpha}{\partial q_\alpha^{h-1} \partial q_\beta^i \partial q_\gamma^j \partial q_\delta^k} \approx \frac{1}{2\Delta} \frac{\partial^{n-2}}{\partial q_\alpha^{h-1} \partial q_\beta^{i-1} \partial q_\gamma^j \partial q_\delta^k} \\
&\quad \times [F_\alpha(q_\beta + \Delta) - F_\alpha(q_\beta - \Delta)] \\
&\approx \frac{1}{4\Delta^2} \frac{\partial^{n-3}}{\partial q_\alpha^{h-1} \partial q_\beta^{i-1} \partial q_\gamma^{j-1} \partial q_\delta^k} [F_\alpha(q_\beta + \Delta, q_\gamma + \Delta) \\
&\quad - F_\alpha(q_\beta - \Delta, q_\gamma + \Delta) - F_\alpha(q_\beta + \Delta, q_\gamma - \Delta) \\
&\quad + F_\alpha(q_\beta - \Delta, q_\gamma - \Delta)] \approx \cdots \\
&= \frac{1}{(2\Delta)^{n-1}} \sum_{n_\alpha=0}^{h-1} \sum_{n_\beta=0}^{i} \sum_{n_\gamma=0}^{j} \sum_{n_\delta=0}^{k} \binom{h-1}{n_\alpha} \binom{i}{n_\beta} \binom{j}{n_\gamma} \binom{k}{n_\delta} \\
&\quad \times (-1)^{n_\alpha + n_\beta + n_\gamma + n_\delta} F_\alpha(q_\alpha + (h - 1 - 2n_\alpha)\Delta, q_\beta \\
&\quad + (i - 2n_\beta)\Delta, q_\gamma + (j - 2n_\gamma)\Delta, q_\delta + (k - 2n_\delta)\Delta),
\end{aligned} \tag{23}$$

where $\alpha, \beta, \gamma, \delta$ label both the atom and the displacement vector, $n = h + i + j + k$ which labels the order of the derivative, F is force, and Δ is the finite difference displacement. For a third order term, four DFT computations will be needed, while eight will be needed for a fourth order term.

The forces are computed within the framework of density functional theory which is carried out using the generalized gradient approximation (GGA) by Perdew and Wang [37] as implemented in the Vienna *ab initio* simulation package (VASP) [38–42]. Γ-centered k meshes depending on the supercell size are applied and a $3 \times 3 \times 3$ mesh is used for the smallest 64-atom supercell. Charge self-consistency is performed until the energy is converged to within 10^{-5} eV, and a plane wave cutoff of 175–350 eV was used depending on the particular computation. Spin-orbit coupling was not utilized.

In order to be sure the direct coefficients are robustly computed within finite difference, one must test for convergence with respect to the displacement size Δ in addition to the supercell size. If Δ is chosen to be too small, a prohibitive plane wave cutoff and k-point mesh will be required, while if it is too large higher order terms will taint the computation. Therefore, there will be an optimum Δ which will be both efficient and accurate, and this will strongly depend on the order of the derivative. In order to illustrate this point, the values of two different fourth order expansion coefficients are plotted as a function of Δ (see Fig. 4). A clear plateau emerges in both cases, revealing a robust value for Δ. After examining a wide range of different types of direct coefficients, we found that $\Delta = 0.01$ Å is reliable for third order, while $\Delta = 0.07$ Å is reliable for fourth order. Supercell size must also be studied to be sure that images are not interacting with one another. The minimum supercell dimension that was used was twice the conventional (i.e., cubic) cell size, while the maximum was six times the conventional cell size. In order to illustrate this, we plot two fourth order coefficients as a function of unit cell size along a particular dimension (see Fig. 5), demonstrating that the changes in the coefficients are diminishing with increasing cell size. Our convergence criteria for supercell dimension was determined based on the largest finite difference coefficient at

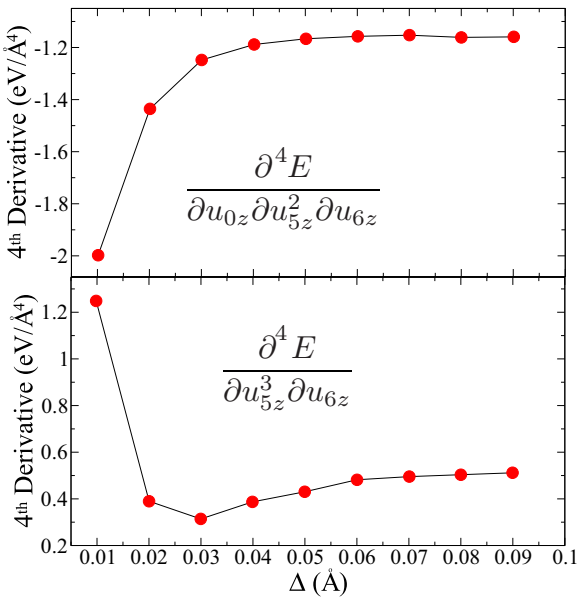

FIG. 4. (Color online) Fourth order derivatives computed using central step finite difference as a function of Δ for a conventional supercell choice of $2 \times 2 \times 3$ (i.e., 96 atoms).

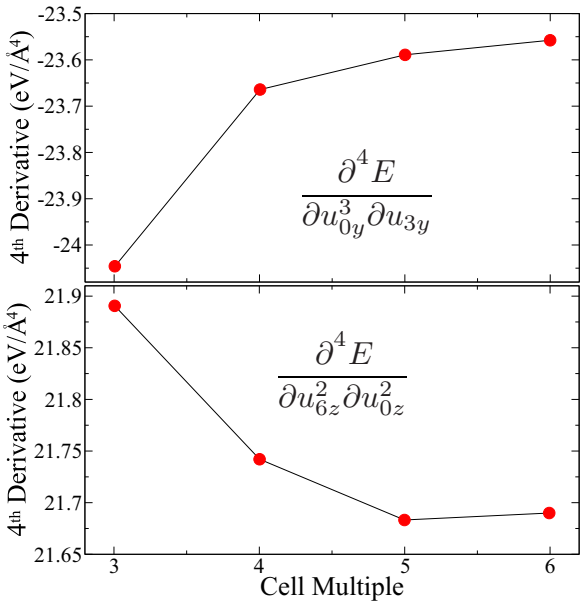

FIG. 5. (Color online) Fourth order derivatives computed using central step finite difference as a function of conventional supercell size in the y direction (top panel) and the z direction (bottom panel) for $\Delta = 0.07$ Å.

a specific order, and for third order the unit cell size was increased until changes were within 0.01 eV/Å^3 while the threshold was 0.1 eV/Å^4 for fourth order.

B. Slave mode expansion coefficients

We have computed 70 direct expansion coefficients at third order and 427 at fourth order. This exceeds the 56 slave mode coefficients at third order and 302 coefficients at fourth order, and therefore we have an overdetermined set of equations. Singular value decomposition can then be used to find the optimum solution in terms of least squares, and this will yield a unique solution for the slave mode coefficients. The third and fourth order terms are plotted in Fig. 6. At third order, the Pb-centered slave modes have substantially larger coefficients than the Te-centered slave modes, while the differences are less pronounced for fourth order. The values of each slave mode coefficient are also listed in Tables I and II.

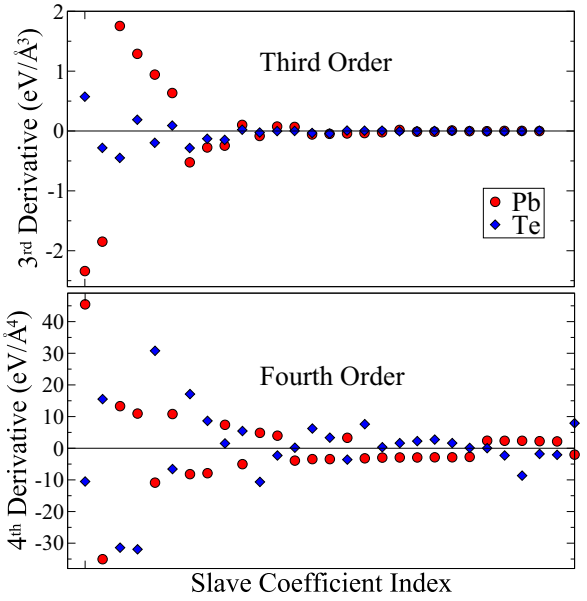

FIG. 6. (Color online) A plot of the third and fourth order slave mode product coefficients Φ. The values are ordered in decreasing magnitude for the Pb-centered coefficients, and the same absolute ordering is used for the Te-centered coefficients. Only a fraction of the fourth order terms are shown for clarity.

V. ASSESSING THE EXPANSION

Having computed the slave mode expansion coefficients up to fourth order and within next-nearest neighbor interaction, we now evaluate the overall reliability of our expansion. The major point of concern in the method we have employed to compute the slave mode coefficients is whether or not the slave mode expansion is sufficiently converged within the octahedron or if non-negligible terms beyond the octahedron are present. A potent test to address this issue is to use the slave mode expansion to compute energy, stress, and phonons as a function of lattice strain. It should be emphasized that our slave mode expansion is performed in the absence of any strain, but if our cluster is sufficiently large the expansion will be able to be used to compute the energetics under strain. Given that strain will amplify the coupling to long-range interactions, and that it is straightforward to compute the answer to these tests using DFT, this serves as an ideal test bed for any type of Taylor series expansion in terms of atomic displacements. PbTe is sufficiently polar such that there are long-range fields which will cause a non-negligible splitting of the optical modes near the Γ point. These can be straightforwardly taken into account

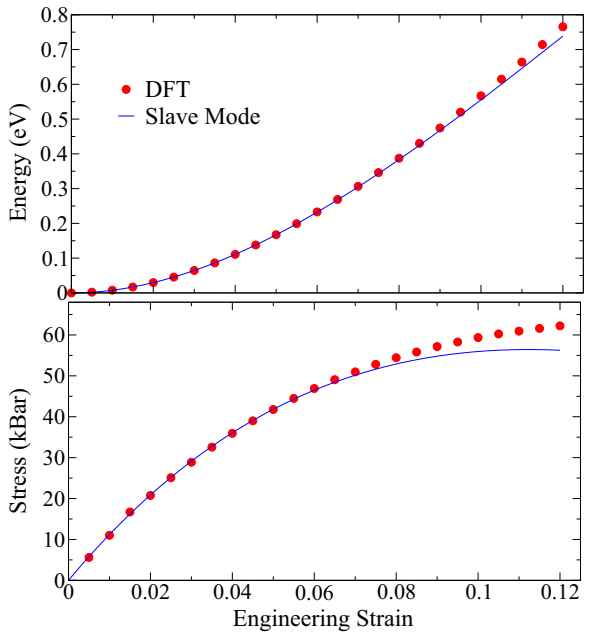

FIG. 7. (Color online) Top panel: Energy as a function of triaxial engineering strain. Bottom panel: True stress as a function of triaxial engineering strain.

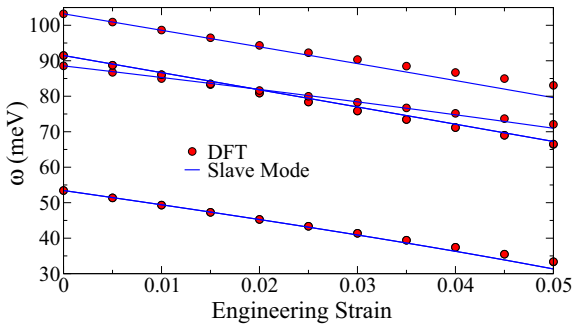

FIG. 8. (Color online) L-point phonon frequencies as a function of triaxial engineering strain.

via Born effective charges [1], but we do not include them in this study.

The first test is to compute the energy and the stress as a function of strain (see Fig. 7). As shown, there is remarkable agreement in the stress for strains as high as 7% and even higher for the energy. At 10% strain there is an error of roughly 8% in the stress. This favorable agreement suggests that longer-range terms are not substantial.

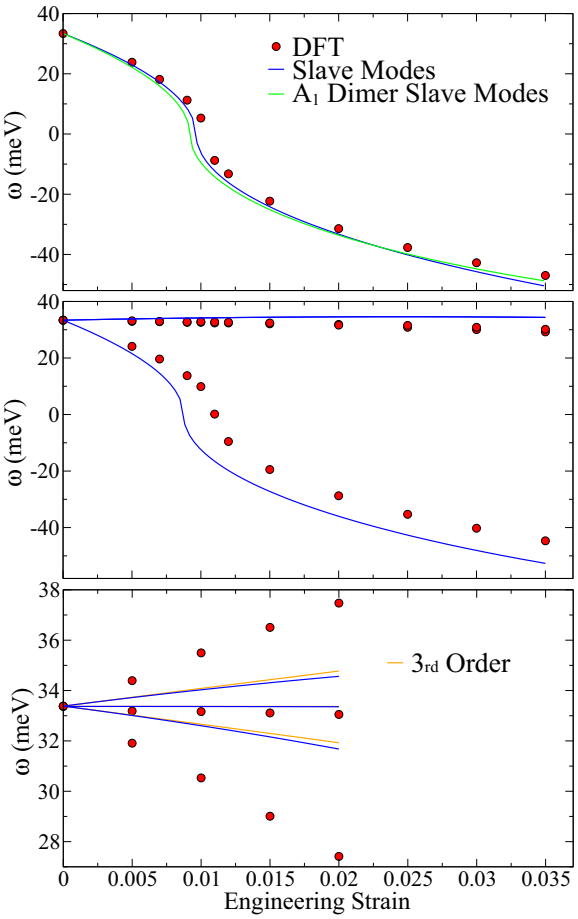

FIG. 9. (Color online) Γ-point optical phonon frequencies as a function of different engineering strain states: triaxial (top panel), uniaxial (middle panel), and shear γ_{xy} (bottom panel). In the top panel, the green curve uses the minimal slave mode expansion which has only two expansion coefficients. In the bottom panel, the orange curve uses only the third order slave mode terms.

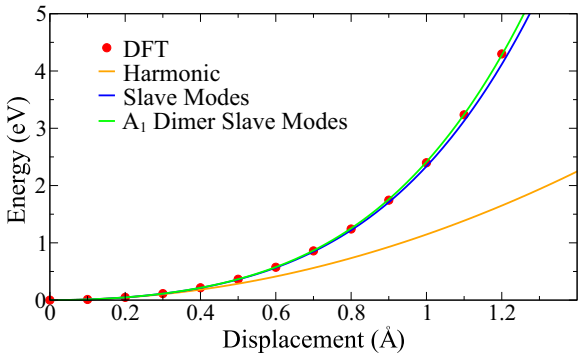

FIG. 10. (Color online) Energy as a function of displacing a single Pb atom in a 216-atom supercell along the $\langle -3,1,1\rangle$ direction. The green curve uses the minimal slave mode expansion which has only two expansion coefficients.

A more stringent test is to compute the phonons as a function of strain. We begin by computing the L-point phonons as a function of strain (see Fig. 8). As shown, there is remarkable agreement up to 5% strain. Another test of phonons under strain is the Γ-point optical modes. This mode is of particular interest in the context of PbTe as it displays anomalous temperature dependence [43–45]. We compute energy of the Γ-point optical modes as a function of triaxial, uniaxial, and shear strain (see Fig. 9). In the case of triaxial strain, the slave mode expansion precisely captures the formation of a soft mode. In the case of uniaxial strain, the slave mode expansion is highly accurate for small strains and properly captures the symmetry breaking of the optical modes. However, errors are apparent for the prediction of the soft mode at larger strains, though the error is relatively constant beyond 1.5%. In the case of shear strain, the splitting of the optical modes is underpredicted using the slave modes, though the error is still within reason in this range of strain. Nonetheless, the troubling aspect of this result is that it does not have the correct slope in the limit of small strains. Given that there is little difference in going from third to fourth order coefficients, this is likely a symptom of longer-range terms that are not present in our expansion. Fortunately, the overall magnitude of this effect is rather small, and these errors will likely be unimportant in most scenarios. The final test will be the displacement of a single Pb atom in a 216-atom supercell (see Fig. 10). The slave mode expansion is highly accurate even at displacements beyond 1.2 Å. We believe these benchmarks demonstrate that our expansion is robust, and it should allow for simulations including both the effects of applied strain in addition to temperature. While some other approaches to the Taylor series expansion isolate the strain modes and treat them separately, the physics of strain is captured in our approach due to the fact that the anharmonic terms have decayed beyond the octahedron.

VI. MINIMAL MODEL

Above we have demonstrated that our slave mode expansion accurately reproduces many key quantities. Nonetheless, it would be strongly desirable if we could somehow extract a *minimal* model of anharmonicity. It would be intuitive

for the nearest-neighbor terms to be larger than the next-nearest-neighbor terms. When choosing the octahedral cluster, the nearest and next-nearest-neighbor terms will be mixed. However, they can be separated. We will start by considering the dimer slave cluster of Pb-Te, where we will use the C_{4v} symmetry along the bond. Given that this case is three dimensional, the representation for the dimer will have six degrees of freedom, and projecting them onto the irreducible representations of the point group yields the following representation: $\Gamma = 2E \oplus 2A_1$. The representation for the modes which shift the dimer in the x,y,z directions can be chosen as one set of $E \oplus A_1$ and this must be removed leaving the following slave mode representation: $E \oplus A_1$. These modes can be explicitly constructed as follows:

$$\phi_{A_1} = \frac{1}{\sqrt{2}}(u_{\mathrm{Te},x} - u_{\mathrm{Pb},x}), \quad \phi_{E^{(1)}} = \frac{1}{\sqrt{2}}(u_{\mathrm{Te},y} - u_{\mathrm{Pb},y}),$$
$$\phi_{E^{(2)}} = \frac{1}{\sqrt{2}}(u_{\mathrm{Te},z} - u_{\mathrm{Pb},z}). \tag{24}$$

In this case we chose a cluster centered on a bond where the x axis aligns with the fourfold rotation axis. At third order there will be two terms: $\phi^3_{A_1}$ and $\phi_{A_1}(\phi^2_{E^{(1)}} + \phi^2_{E^{(2)}})$. At fourth order there will be four terms: $\phi^4_{A_1}$ and $\phi^2_{A_1}(\phi^2_{E^{(1)}} + \phi^2_{E^{(2)}})$ and $\phi^2_{E^{(1)}}\phi^2_{E^{(2)}}$ and $\phi^4_{E^{(1)}} + \phi^4_{E^{(2)}}$. The O_h symmetry center will then generate five more equivalent sets of slave mode products for each case, one for each bond. We can add these terms to our original set of products in Tables I and II, but then we will need to remove two products at third order and four products at fourth order to regain an irreducible space. This is equivalent to performing a unitary transformation within the product space. After reconstructing the expansion coefficients for this new set of products, we then Gram-Schmidt orthogonalize all of the products starting from the dimer mode products. This physically motivated choice of phase convention in the product space achieves the goal of creating a minimal model in that there is now one dominant term at both third and fourth order (see Fig. 11). The dominant terms correspond to $\phi^3_{A_1}$ at third order and $\phi^4_{A_1}$ at fourth order. These two terms can be used to explicitly write a minimal model for the potential (we drop the A_1 index below):

$$V = V_H + \Phi_3 \sum_{\mathbf{R}} \left(-\phi^3_{\mathbf{R}x_-} + \phi^3_{\mathbf{R}x_+} - \phi^3_{\mathbf{R}y_-} + \phi^3_{\mathbf{R}y_+} - \phi^3_{\mathbf{R}z_-} + \phi^3_{\mathbf{R}z_+}\right) + \Phi_4 \sum_{\mathbf{R}} \left(\phi^4_{\mathbf{R}x_-} + \phi^4_{\mathbf{R}x_+} + \phi^4_{\mathbf{R}y_-} + \phi^4_{\mathbf{R}y_+} + \phi^4_{\mathbf{R}z_-} + \phi^4_{\mathbf{R}z_+}\right) \tag{25}$$

and

$$\phi_{\mathbf{R}z_-} = \tfrac{1}{\sqrt{2}}\left(u^{\mathbf{R}+\mathbf{a_1}}_{\mathrm{Te},z} - u^{\mathbf{R}}_{\mathrm{Pb},z}\right), \quad \phi_{\mathbf{R}z_+} = \tfrac{1}{\sqrt{2}}\left(u^{\mathbf{R}+\mathbf{a_2}+\mathbf{a_3}}_{\mathrm{Te},z} - u^{\mathbf{R}}_{\mathrm{Pb},z}\right),$$
$$\phi_{\mathbf{R}x_-} = \tfrac{1}{\sqrt{2}}\left(u^{\mathbf{R}+\mathbf{a_2}}_{\mathrm{Te},x} - u^{\mathbf{R}}_{\mathrm{Pb},x}\right), \quad \phi_{\mathbf{R}x_+} = \tfrac{1}{\sqrt{2}}\left(u^{\mathbf{R}+\mathbf{a_1}+\mathbf{a_3}}_{\mathrm{Te},x} - u^{\mathbf{R}}_{\mathrm{Pb},x}\right),$$
$$\phi_{\mathbf{R}y_-} = \tfrac{1}{\sqrt{2}}\left(u^{\mathbf{R}+\mathbf{a_3}}_{\mathrm{Te},y} - u^{\mathbf{R}}_{\mathrm{Pb},y}\right), \quad \phi_{\mathbf{R}y_+} = \tfrac{1}{\sqrt{2}}\left(u^{\mathbf{R}+\mathbf{a_1}+\mathbf{a_2}}_{\mathrm{Te},y} - u^{\mathbf{R}}_{\mathrm{Pb},y}\right),$$

where V_H is the harmonic part of the potential, ϕ are the slave modes for the dimer, u are the atomic displacements, and $\mathbf{a_i}$ are the primitive lattice vectors of PbTe. There are six dimer slave modes per primitive unit cell, one corresponding to each Pb-Te octahedral bond, and these are simply a displacement difference between corresponding vectors of Pb and Te.

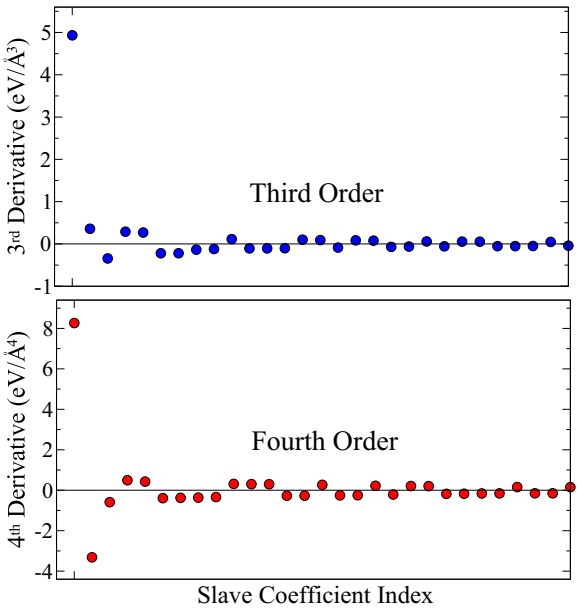

FIG. 11. (Color online) A plot of the transformed third and fourth order slave mode product coefficients Φ'. The values are ordered in decreasing magnitude. Only a fraction of the fourth order coefficients are shown.

The values for the expansion coefficients are found to be $\Phi_3 = 2.68\ \mathrm{eV/\AA^3}$ and $\Phi_4 = 3.70\ \mathrm{eV/\AA^4}$, respectively. The values in Fig. 11 are normalized in the space of monomials in order to have a meaningful relative comparison, whereas the preceding values are consistent with the prefactors in Eq. (25). We can test the reliability of using only these two parameters by recomputing the optical modes under strain (see Fig. 9) and the energy of displacing a single atom (see Fig. 10), displaying excellent agreement with the full expansion. This minimal model has already been used to capture the anomalous temperature dependence of the phonon spectra in PbTe [45]. There is one other term at fourth order which, though smaller, stands out among the other terms. This corresponds to $\phi^2_{A_1}(\phi^2_{E^{(1)}} + \phi^2_{E^{(2)}})$ and has a coefficient of $-1.37\ \mathrm{eV/\AA^4}$. We conclude this section by pointing out that this procedure for constructing a minimal model could be used in any scenario, though it is unclear if it will be as useful.

VII. CONCLUSIONS

In conclusion, we have introduced an approach to perform a Taylor series expansion of the total energy as a function of the nuclear displacements. The novelty of our approach is the formation of new variables (i.e., slave modes) which transform like the irreducible representations of the point group while satisfying the homogeneity of free space, and this approach can be seen as a particular realization of a symmetrized monomial representation of the potential. We used a finite difference approach to compute the slave mode coefficients, and accurately determined all 358 terms within fourth order and next-nearest-neighbor coupling. Examining the energy, stress, and phonons under lattice strain indicated that our expansion parameters are robust and that terms

outside of the octahedron are relatively small. Furthermore, we have introduced an additional approach to perform a unitary transformation which allows us to accurately compress 56 cubic terms to one term and the 302 quartic terms to one term. This two parameter model of anharmonicity in PbTe has already been separately used to compute the temperature dependent phonon spectrum in the classical limit, resolving a major experimental anomaly [45]. Our slave mode expansion should be broadly applicable to highly symmetric materials. While substantial resources have been dedicated to characterizing minimal models of electronic Hamiltonians, much less has been done in terms of characterizing anharmonic phonon interactions of relevant materials. Our approach should make this task substantially more tractable.

ACKNOWLEDGMENTS

C.A.M. and X.A. acknowledge support from the National Science Foundation (Grant No. CMMI-1150795). Y.C. acknowledges support from a Columbia RISE grant.

[1] S. Baroni, S. de Gironcoli, A. Dal Corso, and P. Giannozzi, Rev. Mod. Phys. **73**, 515 (2001).
[2] K. Kunc and R. M. Martin, Phys. Rev. Lett. **48**, 406 (1982).
[3] D. Alfe, Comput. Phys. Commun. **180**, 2622 (2009).
[4] K. Parlinski, Z. Q. Li, and Y. Kawazoe, Phys. Rev. Lett. **78**, 4063 (1997).
[5] A. van de Walle and G. Ceder, Rev. Mod. Phys. **74**, 11 (2002).
[6] M. Born and K. Huang, *Dynamical Theory of Crystal Lattices* (Oxford University Press, New York, 1998).
[7] D. A. Papaconstantopoulos and M. J. Mehl, J. Phys.: Condens. Matter **15**, R413 (2003).
[8] D. R. Bowler and T. Miyazaki, Rep. Prog. Phys. **75**, 036503 (2012).
[9] J. VandeVondele, U. Borstnik, and J. Hutter, J. Chem. Theory .Comput. **8**, 3565 (2012).
[10] G. Kotliar, S. Y. Savrasov, K. Haule, V. S. Oudovenko, O. Parcollet, and C. A. Marianetti, Rev. Mod. Phys. **78**, 865 (2006).
[11] D. Vanderbilt, S. H. Taole, and S. Narasimhan, Phys. Rev. B **40**, 5657 (1989).
[12] R. D. King-Smith and D. Vanderbilt, Phys. Rev. B **49**, 5828 (1994).
[13] W. Zhong, D. Vanderbilt, and K. M. Rabe, Phys. Rev. Lett. **73**, 1861 (1994).
[14] W. Zhong, D. Vanderbilt, and K. M. Rabe, Phys. Rev. B **52**, 6301 (1995).
[15] P. N. Keating, Phys. Rev. **145**, 637 (1966).
[16] P. N. Keating, Phys. Rev. **149**, 674 (1966).
[17] E. Pytte, Phys. Rev. B **5**, 3758 (1972).
[18] K. M. Rabe and U. V. Waghmare, Phys. Rev. B **52**, 13236 (1995).
[19] J. Íñiguez, A. García, and J. M. Pérez-Mato, Phys. Rev. B **61**, 3127 (2000).
[20] K. Esfarjani and H. T. Stokes, Phys. Rev. B **77**, 144112 (2008).
[21] K. Esfarjani, G. Chen, and H. T. Stokes, Phys. Rev. B **84**, 085204 (2011).
[22] J. Shiomi, K. Esfarjani, and G. Chen, Phys. Rev. B **84**, 104302 (2011).
[23] T. Shiga, J. Shiomi, J. Ma, O. Delaire, T. Radzynski, A. Lusakowski, K. Esfarjani, and G. Chen, Phys. Rev. B **85**, 155203 (2012).
[24] J. C. Wojdel, P. Hermet, M. P. Ljungberg, P. Ghosez, and J. Iniguez, J. Phys.: Condens. Matter **25**, 305401 (2013).
[25] J. Behler and M. Parrinello, Phys. Rev. Lett. **98**, 146401 (2007).
[26] H. Eshet, R. Z. Khaliullin, T. D. Kuhne, J. Behler, and M. Parrinello, Phys. Rev. B **81**, 184107 (2010).
[27] H. Eshet, R. Z. Khaliullin, T. D. Kuhne, J. Behler, and M. Parrinello, Phys. Rev. Lett. **108**, 115701 (2012).
[28] R. Z. Khaliullin, H. Eshet, T. D. Kuhne, J. Behler, and M. Parrinello, Nat. Mater. **10**, 693 (2011).
[29] L. J. Nelson, G. L. W. Hart, F. Zhou, and V. Ozoliņš, Phys. Rev. B **87**, 035125 (2013).
[30] J. Cornwell, *Group Theory in Physics* (Academic Press, London, 1997).
[31] M. Tinkham, *Group Theory and Quantum Mechanics* (Dover, Mineola, New York, 1964).
[32] X. F. Zhou and P. Pulay, J. Comput. Chem. **10**, 935 (1989).
[33] X. Gonze and J. P. Vigneron, Phys. Rev. B **39**, 13120 (1989).
[34] A. Debernardi, S. Baroni, and E. Molinari, Phys. Rev. Lett. **75**, 1819 (1995).
[35] G. Deinzer, G. Birner, and D. Strauch, Phys. Rev. B **67**, 144304 (2003).
[36] R. M. Martin, *Electronic Structure: Basic Theory and Practical Methods* (Cambridge University Press, New York, 2008).
[37] J. P. Perdew, J. A. Chevary, S. H. Vosko, K. A. Jackson, M. R. Pederson, D. J. Singh, and C. Fiolhais, Phys. Rev. B **46**, 6671 (1992).
[38] G. Kresse and J. Hafner, Phys. Rev. B **47**, 558 (1993).
[39] G. Kresse and J. Hafner, Phys. Rev. B **49**, 14251 (1994).
[40] G. Kresse and J. Furthmuller, Comput. Mater. Sci. **6**, 15 (1996).
[41] G. Kresse and J. Furthmuller, Phys. Rev. B **54**, 11169 (1996).
[42] G. Kresse and D. Joubert, Phys. Rev. B **59**, 1758 (1999).
[43] K. M. Ø. Jensen, E. S. Božin, C. D. Malliakas, M. B. Stone, M. D. Lumsden, M. G. Kanatzidis, S. M. Shapiro, and S. J. L. Billinge, Phys. Rev. B **86**, 085313 (2012).
[44] O. Delaire, J. Ma, K. Marty, A. F. May, M. A. McGuire, M.-H. Du, D. J. Singh, A. Podlesnyak, G. Ehlers, M. D. Lumsden, and B. C. Sales, Nat. Mater. **10**, 614 (2011).
[45] Y. Chen, X. Ai, and C. A. Marianetti, arXiv:1312.6109.